THE

PHYSICAL REVIEW

A journal of experimental and theoretical physics established by E. L. Nichols in 1893

SECOND SERIES, VOL. 112, NO. 5 DECEMBER 1, 1958

Low-Temperature Behavior of a Dilute Bose System of Hard Spheres. I. Equilibrium Properties*

T. D. LEE† AND C. N. YANG‡
Brookhaven National Laboratory, Upton, New York

(Received August 13, 1958)

By a generalization of the method used in a previous paper the distribution of energy levels of a dilute Bose system of hard spheres is found. These energy levels are then used to compute the statistical properties for the system. A phase transition is found, and the transition point is calculated to the lowest order of a, the diameter of the hard spheres. Furthermore, the thermodynamical functions of the system in both the gas phase and the degenerate phase are obtained, provided $(a/\lambda)\ll 1$ and $\rho a^3 \ll 1$, where λ is the thermal wavelength and ρ is the particle density.

1. INTRODUCTION

IN a recent paper[1] the energy levels of a dilute Bose system of hard spheres near the ground state were calculated using the pseudopotential method.[2] From the distribution of these energy levels, it is possible to calculate the thermodynamic behavior near $T=0$. To extend these considerations to higher excitations and higher temperatures, and especially to investigate the phase transition of the system corresponding to the Bose-Einstein condensation of a free Bose gas is the aim of the present paper.

For the free Bose gas it is well known that between the transition temperature and $T=0$ there is macroscopic but incomplete occupation of the free-particle ground state. It turns out that this possibility of a macroscopic but incomplete occupation of a microscopic state can be incorporated into the method of reference 1. One obtains in this way a calculation which furnishes a natural connection between the concept of the degenerate phase in the sense of London's work[3] and the concept of phonon excitations in the sense of Landau's treatment.[4] The latter is particularly useful in the $T\cong 0$ region, the former at higher temperatures. The dual applicability of both concepts in the present calculation therefore makes possible a discussion of the thermodynamical properties of a dilute (i.e., $\rho a^3 \ll 1$) hard-sphere Bose system at all temperatures for which $a/\lambda \ll 1$, where a is the diameter of the hard spheres, ρ is the particle density, and λ is the thermal wavelength.

The system is found to exist in two thermodynamical phases, which correspond to the two phases of the free Bose gas. In each phase, corrections to the thermodynamical functions to the lowest order of a are obtained. The change in the transition point pressure and density is also obtained. In Sec. 8 a comparison is made between the calculated change of the transition point and the results of the binary collision method.

The method of the present paper for obtaining the excited energy levels can be easily generalized by a Galilean transformation. This will be discussed in a subsequent paper (paper II) and leads to the two-fluid concept[5] and to superfluidity.

If one continues along the line of approximation used in reference 1 and in this paper, one arrives at calculations concerning phonon scatterings and phonon lifetimes, which will be described in detail in future communications.

2. REVIEW

The method used in reference 1 for computing the ground-state energy and the distribution of energy

---

* Work performed under the auspices of the U. S. Atomic Energy Commission.

† Permanent address: Columbia University, New York, New York.

‡ Permanent address: The institute for Advanced Study, Princeton, New Jersey.

[1] Lee, Huang, and Yang, Phys. Rev. **106**, 1135 (1957). We adopt the notation of this paper in the present work.

[2] Kerson Huang and C. N. Yang, Phys. Rev. **105**, 767 (1957).

[3] See, e.g., F. London, *Superfluids II* (John Wiley and Sons, Inc., New York, 1954).

[4] L. D. Landau, J. Phys. U.S.S.R. **5**, 71 (1940).

[5] L. Tisza, J. phys. radium **1**, 164 (1940).

levels near the ground state are based on the following points:

(i) The use of the pseudopotential in higher approximations. This was discussed in detail in reference 2. The crucial point is that the correct pseudopotential

$$V=8\pi a\sum_{i<j}\delta^3(\mathbf{r}_i-\mathbf{r}_j)\frac{\partial}{\partial r_{ij}}(r_{ij}) \tag{1}$$

must be used. If one uses instead

$$V'=8\pi a\sum_{i<j}\delta^3(\mathbf{r}_i-\mathbf{r}_j), \tag{1'}$$

then in higher approximations spurious infinities are encountered. In most computations, however, it is a great practical convenience to use V' first and to switch to V in the end.

(ii) In considering the Hamiltonians (in units $2m=\hbar=1$),

$$\begin{aligned} H&=-\sum\nabla_i^2+V \\ \text{and}\qquad H'&=-\sum\nabla_i^2+V', \end{aligned} \tag{2}$$

one chooses the free-particle representation with periodic boundary conditions. (The importance of choosing the periodic boundary condition was emphasized in reference 1, footnote 17.) An off-diagonal matrix element of

$$V'=\Omega^{-1}4\pi a\sum a_\alpha{}^*a_\beta{}^*a_\mu a_\nu\delta^3(\mathbf{k}_\alpha+\mathbf{k}_\beta-\mathbf{k}_\mu-\mathbf{k}_\nu) \tag{3}$$

then characterizes the collision of two particles of momenta $\mathbf{k}_\mu$, $\mathbf{k}_\nu$ going into the individual particle states with momenta $\mathbf{k}_\alpha$, $\mathbf{k}_\beta$, while all the other particles preserve their momenta. The value of such a matrix element is

$$\Omega^{-1}4\pi a[n_\alpha n_\beta(n_\mu+1)(n_\nu+1)]^{\frac{1}{2}}. \tag{4}$$

Through such matrix elements one mixes states with different free particle occupation numbers. However, we saw in reference 1 that *the states that need be mixed to form an eigenstate of the Hamiltonian have occupation numbers which are the same to the order of N, if the parameter $(\rho a^3)^{\frac{1}{2}}$ is regarded as small.*

We recall in fact that in reference 1 one starts from the free-particle ground state and combines it with other states S that can be reached from the free-particle ground state through a series of off-diagonal elements (4). The assumption is made that all such states S have as the occupation number for the free-particle ground state $n_0\sim N$. This assumption is later justified because to deplete the ground state of $2m$ particles one must go through the off-diagonal elements (4) at least m times. Since a is a small parameter, this gives a small probability for those states S for which n_0 is much different from N. In fact, it was shown that the probability falls off in a geometrical series with increasing m, making it a good approximation to take $n_0\sim N$ for all states S of importance.

(iii) A further simplification occurs when one first drops all the off-diagonal elements (4) except those for which two of the four occupation numbers n_α, n_β, n_μ, n_ν are of the order of a finite fraction of N. The dropped elements are smaller than those kept by a factor of at least $\sim N^{\frac{1}{2}}$. However, there are more of these dropped elements than of those kept by a factor of at least N. It is not immediately obvious that these more numerous smaller matrix elements contribute less than the large off-diagonal elements. This question was discussed in reference 1, where it was shown that by treating these small matrix elements as a perturbation one obtains correction terms in the form of an expansion in powers of the parameter $(\rho a^3)^{\frac{1}{2}}$.

Based on the points reviewed above, calculations were made in reference 1 for those states for which *the occupations of the free particle ground state is essentially complete.* The ground-state energy was found to be

$$E_0=4\pi a\rho N[1+(128/15\sqrt{\pi})(\rho a^3)^{\frac{1}{2}}+O(\rho a^3)]. \tag{5}$$

The excited states near the ground state were shown to have energies and momenta

$$\begin{aligned} E(m_\mathbf{k})&=E_0+\sum_{\mathbf{k}\neq0}m_\mathbf{k}(k^4+16\pi a\rho k^2)^{\frac{1}{2}}, \\ \mathbf{P}(m_\mathbf{k})&=\sum m_\mathbf{k}\mathbf{k}, \end{aligned} \tag{6}$$

where $m_\mathbf{k}$ are any positive integers that satisfy the additional condition

$$N^{-1}\sum_{\mathbf{k}\neq0}m_\mathbf{k}=O(N^{-1}). \tag{7}$$

Furthermore, these states were shown to correspond to states with $m_\mathbf{k}$ quanta of compressional waves with wave number $k/2\pi$.

3. MACROSCOPIC BUT INCOMPLETE OCCUPATION OF THE FREE-PARTICLE GROUND STATE

We shall show now that the method of approximation reviewed in the last section is applicable to states for which there is macroscopic but incomplete occupation of the free-particle ground state, i.e., states for which the free-particle ground state occupation number n_0 is essentially $N\xi$ where ξ is a finite fraction, and for which no other state is occupied by a finite fraction of the N particles.

To discuss such states, we start from a state with the following occupation numbers:

$$\begin{gathered} n_0=n_0{}^0=N\xi, \\ n_\mathbf{k}=n_\mathbf{k}{}^0,\quad N^{-1}n_\mathbf{k}{}^0=O(N^{-1})\quad(\mathbf{k}\neq0), \\ \sum_{\mathbf{k}\neq0}n_\mathbf{k}{}^0=(1-\xi)N. \end{gathered} \tag{8}$$

Similarly to point (ii) of the last section, we need only consider states for which, to the order of N, the occupation number $n_{\mathbf{k}}$ does not drastically differ from $n_{\mathbf{k}}^0$. Writing

$$n_{\mathbf{k}}=n_{\mathbf{k}}^0+\delta_{\mathbf{k}} \quad (\mathbf{k}\neq 0), \tag{9}$$

it is possible to show in the same *a posteriori* manner, as done in Sec. 3 of reference 1 for the problem when $\xi=1$, that

$$\langle\delta_{\mathbf{k}}\rangle=O(1) \quad \text{for} \quad \mathbf{k}\neq 0,$$

and

$$N^{-1}\sum_{\mathbf{k}\neq 0}\langle\delta_{\mathbf{k}}\rangle=O[(\rho a^3)^{\frac{1}{2}}]. \tag{10}$$

The diagonal elements of V' were computed in reference 1:

$$\langle n|V'|n\rangle=\Omega^{-1}4\pi a(2N^2-N-\textstyle\sum_{\mathbf{k}}n_{\mathbf{k}}^2).$$

Using (8) and (9), one can write this as

$$\langle n|V'|n\rangle$$
$$=\Omega^{-1}4\pi a[N^2+(1-\xi)^2N^2+2\xi N\sum_{\mathbf{k}\neq 0}n_{\mathbf{k}}]+V_1, \tag{11}$$

where

$$V_1=-\Omega^{-1}4\pi a[N+\sum_{\mathbf{k}\neq 0}n_{\mathbf{k}}^2+(\sum_{\mathbf{k}\neq 0}\delta_{\mathbf{k}})^2] \tag{12}$$

will be neglected because (10) shows that its contribution is of higher orders in $(\rho a^3)^{\frac{1}{2}}$. One then has

$$\langle n|V'|n\rangle=4\pi a\rho N[1+(1-\xi)^2]+8\pi a_n\xi\sum_{\mathbf{k}\neq 0}a_{\mathbf{k}}{}^*a_{\mathbf{k}}$$
$$+\text{negligible terms.} \tag{13}$$

To discuss the off-diagonal matrix elements of V' we take advantage of the simplification discussed in point (iii) of the last section. We keep, therefore, only those off-diagonal elements that correspond to a collision of two particles with momenta 0, going into momenta states $\mathbf{k}$ and $-\mathbf{k}$ or vice versa. All states that can be reached from the state (8) by such off-diagonal elements have the same value for $(n_{\mathbf{k}}-n_{-\mathbf{k}})=(n_{\mathbf{k}}^0-n_{-\mathbf{k}}^0)$.

It is not difficult to see that for these states the Hamiltonian assumes a form very similar to that discussed in reference 1 (which in fact is a special case of the present problem corresponding to $\xi=1$).

$$H'=4\pi a\rho N[1+(1-\xi)^2]+2\sum{}'a_{\mathbf{k}}{}^*a_{\mathbf{k}}(k^2+8\pi a\xi\rho)$$
$$+\sum{}'8\pi a\xi\rho B_{S(\mathbf{k})}(\mathbf{k}), \tag{14}$$

where the $\sum'$ extends over half of the $\mathbf{k}$ space excluding $\mathbf{k}=0$, $S(\mathbf{k})=|n_{\mathbf{k}}^0-n_{-\mathbf{k}}^0|$, and $B_S(\mathbf{k})$ is defined in Eq. (A3) of reference 1. It is important to notice that $B_S(\mathbf{k})$ and $B_S(\mathbf{k}')$ for different $\mathbf{k}$ and $\mathbf{k}'$ operate on different occupation numbers, and therefore commute with each other.

Equation (14) can be written as

$$H'=4\pi a\rho N[1+(1-\xi)^2]$$
$$+2\sum{}'(k^2+8\pi a\xi\rho)[a_{\mathbf{k}}{}^*a_{\mathbf{k}}+y_{\mathbf{k}}'B_{S(\mathbf{k})}(\mathbf{k})], \tag{15}$$

where

$$y_{\mathbf{k}}'=(k^2+8\pi a\xi\rho)^{-1}4\pi a\xi\rho.$$

The individual terms in the summation in (15) commute and can be simultaneously diagonalized.

The eigenfunctions and the eigenvalues of these terms have been evaluated in the Appendix of reference 1. As remarked in Sec. 2, calculation of the energy levels using V' lead to spurious terms which are divergent. The substitution of the true pseudopotential V for the V' lead to the correct final answer for the energy spectrum. Following arguments which run exactly parallel to that of reference 1, we find the energy spectrum to be

$$E(\xi,m_{\mathbf{k}})=E_0(\xi)+E_{\text{phonon}}(\xi), \tag{16}$$

where

$$E_0(\xi)=4\pi a\rho N[1+(1-\xi)^2$$
$$+(128/15\sqrt{\pi})(\rho a^3\xi^3)^{\frac{1}{2}}+O(\rho a^3)], \tag{17}$$

and

$$E_{\text{phonon}}(\xi)=\sum_{\mathbf{k}\neq 0}m_{\mathbf{k}}k(k^2+16\pi a\xi\rho)^{\frac{1}{2}}. \tag{18}$$

Here $m_{\mathbf{k}}$ are positive integers satisfying

$$N^{-1}\sum_{\mathbf{k}\neq 0}m_{\mathbf{k}}=(1-\xi)+O(N^{-1}). \tag{19}$$

The momentum of the system in the state specified by ξ, $m_{\mathbf{k}}$ is

$$\mathbf{P}(\xi,m_{\mathbf{k}})=\sum m_{\mathbf{k}}\mathbf{k}. \tag{20}$$

We remark that for $\xi=1$, these results reduce to those obtained in reference 1. It is furthermore important to remember that these equations do not give correct results to the order a, unless $ka\ll 1$, which is a condition for the applicability of the pseudopotential.

The physical interpretation of (16), (17), and (18) is exactly the same as before: $m_{\mathbf{k}}$ is the number of elementary excitons with wave number $(k/2\pi)$. One notices, however, that the energy of the excitation is now $(k^2+16\pi a\xi\rho)^{\frac{1}{2}}k$ which depends on ξ. For $\xi\neq 0$, this excitation energy varies linearly with k for small k and represents phonons. For $\xi=0$, the excitations assume the character of individual particle excitations.

The parameter ξ is, according to the spirit of the calculation above, the fraction of particles that are in the unperturbed ground state [neglecting terms of $O(\rho a^3)^{\frac{1}{2}}$]. Also the fraction $1-\xi$ is, according to (19), the ratio of the total number of excitations to the total number of particles. That the two are related is a natural consequence of the method of approach adopted above. It is perhaps worth emphasizing that the present calculation thus provides, in the model under discussion, a link between the two different viewpoints that have greatly influenced the development of our understanding of He II: the concept of the degenerate occupation of a single state, which led to London's proposal[3] that the λ transition in He is a consequence of Bose-Einstein condensation, and the concept of elementary phonon excitations, which led to Landau's theory[4] of liquid He. The dual applicability of both concepts in the present calculation also enables us to carry out calculations at all temperatures, including both the transition region and the region near $T=0$. In a subsequent paper where transport phenomena are discussed it will become clear that the parameter ξ corresponds to the fraction of superfluid, a concept first phenomenologically introduced by Tisza.[5]

The two terms $E_0(\xi)$ and $E_{\text{phonon}}(\xi)$ in (16) are accurate to the order of N (and not 1), which is sufficient for the calculation of the thermodynamical properties of the system. However, from the derivation it is clear that (16) can also be used to compute the energy difference (which is of the order of 1) between two states for which there is only a difference in a finite number of $m_{\mathbf{k}}$'s. For example, two states with a difference of one phonon belong in this computation to the *same* value of ξ and consequently their energy difference is

$$k(k^2+16\pi a\rho\xi)^{\frac{1}{2}},$$

which is of the order of 1.

4. PARTITION FUNCTION

Using the energy spectrum, Eqs. (16)–(19), we proceed to calculate the partition function Q for a dilute system of hard spheres obeying Bose statistics. We first define

$$Q(\xi)=\sum_{m_{\mathbf{k}}}\exp[-\beta E(\xi,m_{\mathbf{k}})], \tag{21}$$

where β is related to the Boltzmann constant κ and the temperature T by

$$\beta=(\kappa T)^{-1}, \tag{22}$$

and the sum over $m_{\mathbf{k}}$ extends over all positive integral values provided

$$N^{-1}\sum_{\mathbf{k}\neq 0} m_{\mathbf{k}}=(1-\xi). \tag{23}$$

The partition function Q is a sum of $Q(\xi)$ over all allowable ξ's. However, for an infinite sytem ($N\rightarrow\infty$, but keeping ρ finite) the logarithm of Q is replaceable by the maximum of $\ln Q(\xi)$ with respect to ξ.

$$\ln Q(\bar{\xi})=\ln Q, \tag{24}$$

where the most probable value $\bar{\xi}$ is determined by the condition

$$\ln Q(\bar{\xi})=\text{maximum}[\ln Q(\xi)], \tag{25}$$

for all values of ξ between 0 and 1.

The quantity $\ln Q(\xi)$ can be readily evaluated by means of the method of steepest descent. We have

$$-\kappa T\Omega^{-1}\ln Q(\xi)=f(\xi,\zeta),$$

where

$$f(\xi,\zeta)=4\pi a\rho^2[1+(1-\xi)^2]+(1-\xi)\kappa T\rho\ln\zeta$$
$$+(8\pi^3)^{-1}\kappa T\int\ln(1-\zeta e^{-\beta\omega})d^3k. \tag{26}$$

The parameter ζ is related to ξ by

$$(\partial f/\partial\zeta)_\xi=0,$$

i.e.,

$$(1-\xi)\rho=(8\pi^3)^{-1}\int\left(\frac{\zeta e^{-\beta\omega}}{1-\zeta e^{-\beta\omega}}\right)d^3k,\quad(0\leqq\zeta\leqq 1). \tag{27}$$

The quantity ω is given by

$$\omega=k(k^2+16\pi a\xi\rho)^{\frac{1}{2}}. \tag{28}$$

Equation (27) is the condition for steepest descent. We notice that the free energy per unit volume takes the *maximum* value of the function $f(\xi,\zeta)$ with respect to ζ. In Eq. (26), as in all subsequent calculations, we neglect terms of higher powers in $(\rho a^3)^{\frac{1}{2}}$.

It is convenient to introduce a $\xi-\zeta$ plot in which, for fixed T and fixed ρ, ξ is plotted against ζ as a graphical representation of (27). Along each curve one locates the most probable (i.e., equilibrium) ξ by *minimizing* f. For orientation purposes one first investigates the case of free Bose particles (i.e., $a=0$). At fixed T the locus of the equilibrium points in the graph is easily seen to be the curve $OBCDE$ in Fig. 1.

To investigate the change in these equilibrium points brought about by the introduction of the hard-sphere interaction, we notice that *along* the $\xi-\zeta$ curves, one has

$$\frac{df}{d\xi}=\left(\frac{\partial f}{\partial\xi}\right)_\zeta=-\kappa T\rho\ln\zeta$$
$$-a\rho\pi^{-2}\int\frac{\zeta e^{-\beta\omega}}{1-\zeta e^{-\beta\omega}}(1-k^2\omega^{-1})d^3k. \tag{29}$$

We take a point P along the curve $OBCDE$ and study the locus of this point at fixed T and ρ for infinitesimal values of a. [It is important to notice that the extension of this neighborhood is nonuniform in P.] It is convenient to divide the curve $OBCDE$ into three sections:

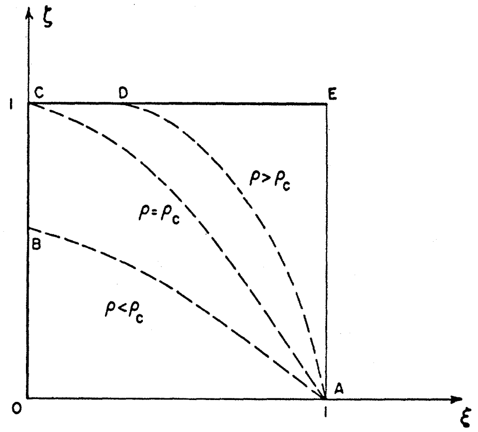

FIG. 1. Schematic $\zeta-\xi$ plots for a free Bose-Einstein gas. The dashed curves AB, AC, and AD represent the relation $(1-\xi)\rho=\lambda^{-3}g_{\frac{3}{2}}(\zeta)$ [Eq. (27) with $a=0$] for the same value of λ but different ρ. $\rho_c=\lambda^{-3}(2.612)$. Curve $OBCDE$ represents the locus of the equilibrium points for the free Bose gas, determined by Eq. (25).

(i) P is in the section OC open at C. For sufficiently small values of a the general shape of the $\xi-\zeta$ curves follow their counterparts in the case of $a=0$. Furthermore, for $a=0$, by (29), the value of $df/d\xi$ along any curve AB in Fig. 1 is always bigger than $-\rho\kappa T\ln(\zeta)_B$ which is positive. For sufficiently small values of a, therefore, $df/d\xi$ remains positive and the minimum of f occurs always at $\xi=0$. Thus the locus of equilibrium points remains along OC (open at C). In algebraic language this means that

$$\bar{\xi}=0. \tag{30}$$

(ii) P is in the section CE open at C. To find the equilibrium value of ξ we must solve the equations $df/d\xi=0$ and (27) for ξ and ζ. It follows from (29) that for $df/d\xi=0$,

$$\zeta=1-O[(\rho a^3)^{\frac{1}{2}}]. \tag{31}$$

Substituting this into (27), one obtains

$$1-\bar{\xi}=(2.612)(\rho\lambda^3)^{-1}-8\left(\frac{a\bar{\xi}}{\pi\rho\lambda^4}\right)^{\frac{1}{2}}+O(a\rho\lambda^2), \tag{32}$$

where

$$\lambda=(4\pi/\kappa T)^{\frac{1}{2}}.$$

The equilibrium point $\bar{\xi}-\zeta$ thus follows a curve slightly below the line CE in Fig. 1.

(iii) P is at C. This is the region near the transition point in which the behavior of a model satisfying strictly the spectrum (16)–(19) is very complicated. It will be discussed in detail in the Appendix.

In the gas region (i) and the degenerate region (ii) it is straightforward to substitute the equilibrium conditions (30), (31), and (32) into (26) and obtain the free energy of the system. The results are summarized in the next two sections.

5. GASEOUS PHASE

This is the phase satisfying $\bar{\xi}=0$. The Helmholtz free energy F_g for the system is given by

$$\Omega^{-1}F_g=-\lambda^{-3}\kappa T g_{\frac{5}{2}}(\zeta)+\rho\kappa T\ln\zeta \\ +8\pi a\rho^2+O[a^{\frac{3}{2}}\lambda^{-13/2}], \tag{33}$$

where the parameter ζ is related to ρ through

$$\rho=\lambda^{-3}g_{\frac{3}{2}}(\zeta), \tag{34}$$

and

$$g_n(\zeta)=\sum_{l=1}^{\infty} l^{-n}\zeta^l. \tag{35}$$

Correspondingly, the energy E_g, entropy S_g, pressure p_g, and specific heat $(C_v)_g$ and the compressibility $(\partial p_g/\partial\rho)^{-1}$ are given by

$$\Omega^{-1}E_g=\tfrac{3}{2}\lambda^{-3}\kappa T g_{\frac{5}{2}}(\zeta)+8\pi a\rho^2, \tag{36}$$

$$\Omega^{-1}S_g=\tfrac{5}{2}\lambda^{-3}\kappa g_{\frac{5}{2}}(\zeta)-\rho\kappa\ln\zeta, \tag{37}$$

$$p_g=\lambda^{-3}\kappa T g_{\frac{5}{2}}(\zeta)+8\pi a\rho^2, \tag{38}$$

$$(\Omega^{-1}C_v)_g=(15/4)\lambda^{-3}\kappa g_{\frac{5}{2}}(\zeta)-(9/4)\kappa\rho g_{\frac{3}{2}}(\zeta)[g_{\frac{1}{2}}(\zeta)]^{-1}, \tag{39}$$

and

$$(\partial p_g/\partial\rho)_T=4\pi\rho\lambda[g_{\frac{1}{2}}(\zeta)]^{-1}+16\pi a\rho. \tag{40}$$

6. DEGENERATE PHASE

In this phase, (31) and (32) obtain. The thermodynamical functions can again be calculated by using the results obtained in Sec. 4 provided

$$\rho a^3\ll 1 \quad\text{and}\quad (a/\lambda)\ll 1. \tag{41}$$

In the following, we list the explicit forms of the thermodynamical functions for this dilute system at moderate temperature $a\rho\lambda^2\ll 1$, [case (i)], at fairly low temperature $a\rho\lambda^2\sim 1$ [case (ii)], and at very low temperature $a\rho\lambda^2\gg 1$, [case (iii)].

(i) The Helmholtz free energy F_d in the degenerate phase for $(\rho a^3)\ll 1$ and $a\rho\lambda^2\ll 1$ is given (neglecting terms proportional to $a^{\frac{3}{2}}$) by

$$\Omega^{-1}F_d=-(1.342)\lambda^{-3}\kappa T+4\pi a(\rho^2+2\rho\rho_c-\rho_c^2), \tag{42}$$

where

$$\rho_c=(2.612)\lambda^{-3}. \tag{43}$$

The other thermodynamical functions are given by

$$\Omega^{-1}E_d=\tfrac{3}{2}(1.342)\lambda^{-3}\kappa T+4\pi a(\rho^2-\rho\rho_c+2\rho_c^2), \tag{44}$$

$$\Omega^{-1}S_d=\tfrac{5}{2}(1.342)\lambda^{-3}\kappa+3\kappa a\lambda^2(\rho_c^2-\rho\rho_c), \tag{45}$$

$$p_d=(1.342)\lambda^{-3}\kappa T+4\pi a(\rho^2+\rho_c^2), \tag{46}$$

$$\Omega^{-1}(C_v)_d=(15/4)(1.342)\lambda^{-3}\kappa+\tfrac{3}{2}\kappa a\lambda^2(4\rho_c^2-\rho\rho_c) \tag{47}$$

and

$$(\partial p_d/\partial\rho)_T=8\pi a\rho. \tag{48}$$

(ii) At much lower temperature $a\rho\lambda^2\sim 1$ but $\rho a^3\ll 1$, the Helmholtz free energy becomes

$$\Omega^{-1}F_d=4\pi a\rho^2[1-4(2\rho a^3)^{\frac{1}{2}}t^{-1}\mathcal{G}(t)+O(\rho a^3)], \tag{49}$$

where

$$t=2a\rho\lambda^2, \tag{50}$$

and

$$\mathcal{G}(t)=-\frac{2}{\sqrt{\pi}}\int_0^\infty x\ln(1-e^{-tx})\left[\frac{(x^2+1)^{\frac{1}{2}}-1}{x^2+1}\right]^{\frac{1}{2}}dx. \tag{51}$$

The series expansion of $\mathcal{G}(t)$ for small and large values of t are given by

$$\mathcal{G}(t)=1.342t^{-\frac{3}{2}}-2.612t^{-\frac{1}{2}} \\ +\tfrac{4}{3}(2\pi)^{\frac{1}{2}}-\tfrac{3}{2}(1.460)t^{\frac{1}{2}}+\cdots, \tag{52}$$

and

$$\mathcal{G}(t)=(2/\pi)^{\frac{1}{2}}\left[\frac{\pi^4}{45t^3}-\frac{\pi^6}{63t^5}+\cdots\right], \tag{53}$$

respectively. For intermediate values of t, $\mathcal{G}(t)$ can be evaluated numerically.

The other thermodynamical functions are given [neglecting terms of higher orders in (ρa^3)] by

$$\Omega^{-1}E_d = 4\pi a\rho^2[1-4(2\rho a^3)^{\frac{1}{2}}d\mathcal{G}/dt], \tag{54}$$

$$\Omega^{-1}S_d = \kappa(2a\rho)^{\frac{3}{2}}[\mathcal{G}-td\mathcal{G}/dt], \tag{55}$$

$$p_d = 4\pi a\rho^2[1-2(2\rho a^3)^{\frac{1}{2}}(t^{-1}\mathcal{G}+2d\mathcal{G}/dt)], \tag{56}$$

and

$$\Omega^{-1}(C_v)_d = \kappa(2a\rho)^{\frac{3}{2}}t^2d^2\mathcal{G}/dt^2. \tag{57}$$

In this low-temperature range, Eq. (32) is not useful; instead one obtains from (27)

$$(1-\bar{\xi})\rho = (2a\rho)^{\frac{3}{2}}\mathfrak{F}(t), \tag{58}$$

where

$$\mathfrak{F}(t) = \frac{2}{\sqrt{\pi}}\int_0^\infty \frac{x}{e^{tx}-1}\left[\frac{(x^2+1)^{\frac{1}{2}}-1}{x^2+1}\right]^{\frac{1}{2}}dx. \tag{59}$$

For small values of t

$$\mathfrak{F}(t) = 2.612t^{-\frac{3}{2}} - 4(2/\pi)^{\frac{1}{2}}t^{-1} + 1.460t^{-\frac{1}{2}} - \cdots, \tag{60}$$

and for large values of t

$$\mathfrak{F}(t) = (2/\pi)^{\frac{1}{2}}[(2.404)t^{-3} - (15.5535)t^{-5} + \cdots]. \tag{61}$$

(iii) In the extremely low temperature region $a\rho\lambda^2 \gg 1$ (but $\rho a^3 \ll 1$), the Helmholtz free energy becomes

$$\Omega^{-1}F_d = 4\pi a\rho^2\left[1-\frac{1}{90}\left(\frac{a}{\lambda}\right)\left(\frac{\pi}{a\rho\lambda^2}\right)^{7/2}\right]. \tag{62}$$

The other thermodynamical functions are

$$\Omega^{-1}E_d = 4\pi a\rho^2\left[1+\frac{1}{30}\left(\frac{a}{\lambda}\right)\left(\frac{\pi}{a\rho\lambda^2}\right)^{7/2}\right], \tag{63}$$

$$\Omega^{-1}S_d = \frac{2}{45}\pi\rho\kappa\left(\frac{a}{\lambda}\right)\left(\frac{\pi}{a\rho\lambda^2}\right)^{5/2}, \tag{64}$$

$$p_d = 4\pi a\rho^2\left[1+\frac{1}{36}\left(\frac{a}{\lambda}\right)\left(\frac{\pi}{a\rho\lambda^2}\right)^{7/2}\right], \tag{65}$$

and

$$\Omega^{-1}(C_v)_d = \frac{2\pi}{15}\rho\kappa\left(\frac{a}{\lambda}\right)\left(\frac{\pi}{a\rho\lambda^2}\right)^{5/2}. \tag{66}$$

At these very low temperatures, $\bar{\xi}$ is given by

$$1-\bar{\xi} = \frac{1.202}{\rho\lambda^3\sqrt{\pi}}\left(\frac{1}{a\rho\lambda^2}\right)^{\frac{3}{2}}. \tag{67}$$

It is interesting to notice that in both the gas region and the degenerate region at moderate temperatures, (i.e., $a\rho\lambda^2 \ll 1$) the thermodynamical functions listed above, to the order included, are the same as the results of a calculation by Huang, Yang, and Luttinger.[6] This is not really surprising because the relevant excitations in these regions have momenta $k \sim \lambda^{-1} \gg (a\rho)^{\frac{1}{2}}$. The spectrum (18) used in the present paper than reduces to

$$E_{\text{phonon}}(\xi) \cong \sum_{\mathbf{k}\neq 0} m_{\mathbf{k}}k^2 + \sum_{\mathbf{k}\neq 0} m_{\mathbf{k}}8\pi a\xi\rho$$
$$= \sum_{\mathbf{k}\neq 0} m_{\mathbf{k}}k^2 + N8\pi a\rho\xi(1-\xi), \tag{68}$$

which, when added to (17), gives

$$E(\xi, m_{\mathbf{k}}) \cong 4\pi aN\rho(2-\xi^2) + \sum_{\mathbf{k}\neq 0} m_{\mathbf{k}}k^2. \tag{69}$$

This formula is exactly identical with the spectrum from which reference 6 starts. It differs from the spectrum (16)–(19) of the present paper because it does not take into account the off-diagonal elements of the potential in Eq. (1). One concludes that for the temperature region under discussion in this paragraph, these off-diagonal elements do not lead to important contributions.

The situation is completely different, however, for the very low temperature region [case (ii) and case (iii) above] which is characterized by phonon excitation with long wavelengths. One observes, for example, that in the degenerate phase C_v varies at moderate temperatures as $T^{\frac{3}{2}}$, but at extremely low temperatures as T^3. This difference of temperature dependence stems from the fact that for long wavelengths the phonon energy is linear instead of quadratic in the momentum. We shall see in a subsequent paper that this change of the energy spectrum is also responsible for the superfluidity of the system.

7. PHASE TRANSITION

By comparing the thermodynamical functions for the two phases, one finds that the phase transition occurs at

$$\lambda^3 p_c/\kappa T = 1.342 + 2(2.612)^2(a/\lambda) + O[(a/\lambda)^{\frac{3}{2}}], \tag{70}$$

and

$$\lambda^3\rho_c = 2.612 + O[a/\lambda], \tag{71}$$

where p_c and ρ_c are the pressure and density or densities at the transition point. It is important to notice that to the order $(a/\lambda)^{\frac{1}{2}}$ there is no discontinuity in density at the transition point. However, *this does not mean that in higher orders there will be no discontinuity in the densities of the two phases*. Similarly one sees that to the order (a/λ) there is no discontinuity in entropy, and to the order that we have calculated there is a discontinuity in the specific heat and a discontinuity in the compressibility. These discontinuities[7] are given by

---

[6] Huang, Yang, and Luttinger, Phys. Rev. **105**, 776 (1957).

[7] The exact meaning of (72) is as follows: Consider $(C_v)_d$ and $(C_v)_g$ as functions of T, ρ, and a. Then

$$\lim_{\rho\to\rho_c+}\ \lim_{a\to 0+}(C_v)_d - \lim_{\rho\to\rho_c-}\ \lim_{a\to 0+}(C_v)_g = 0,$$

and

$$\lim_{\rho\to\rho_c+}\ \lim_{a\to 0+}\frac{\partial(C_v)_d}{\partial a} - \lim_{\rho\to\rho_c-}\ \lim_{a\to 0+}\frac{\partial(C_v)_g}{\partial a} = \frac{9}{2}(2.612)\lambda^{-1}N\kappa.$$

Similarly one can write down the exact meanings of (73). In these equations the order of the two limits $\rho \to \rho_c$ and $a \to 0$ may not be exchanged. Consequently it is not possible to state the exact order of the transition for a finite a.

$$(C_v)_d-(C_v)_g=(9/2)(2.612)(a/\lambda)N\kappa, \tag{72}$$

and

$$\left(\frac{\partial p}{\partial \rho}\right)_d-\left(\frac{\partial p}{\partial \rho}\right)_g=-8\pi a\rho_c \tag{73}$$

at the transition point.

These properties are illustrated by Fig. 2 and Fig. 3.

8. COMPARISON WITH BINARY COLLISION METHOD

The thermodynamical functions in the gaseous phase and the transition point have previously been calculated by a different approach using the binary collision method.[8] The results, of course, agree with that obtained by the present method. It is of interest to compare these two different approaches.

First we compare the present results with the virial type expansion for the gaseous phase displayed in reference 8:

$$\lambda^3 p/\kappa T=g_{\frac{5}{2}}(z)-2(a/\lambda)[g_{\frac{3}{2}}(z)]^2+8(a/\lambda)^2[g_{\frac{3}{2}}(z)]^2 g_{\frac{1}{2}}(z) +8(a/\lambda)^2F(z)+O[(a/\lambda)^3], \tag{74}$$

where

$$\rho=\frac{\partial}{\partial \ln z}\left(\frac{p}{\kappa T}\right), \tag{75}$$

z is the fugacity, and $F(z)$ is

$$F(z)=\sum_{r,s,t=1}^{\infty}\frac{z^{r+s+t}}{(rst)^{\frac{1}{2}}(r+s)(r+t)}. \tag{76}$$

We remark that if we set

$$\ln z=\ln\zeta+4(a/\lambda)g_{\frac{3}{2}}(\zeta)+O[(a/\lambda)^2], \tag{77}$$

then, neglecting $O[(a/\lambda)^2]$, (74) and (75) are identical with (38) and (34). That (77) holds is to be anticipated since the parameter ζ was introduced in (27) in a steepest-descent calculation while the fugacity z is defined by

$$(\partial/\partial N)[\ln Q+N\ln z]=0. \tag{78}$$

A comparison of (78) and (27) leads immediately to (77).

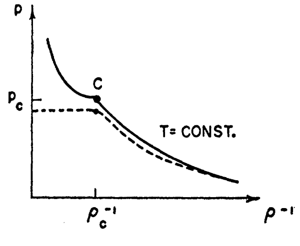

FIG. 2. Schematic $p-V$ diagram for a dilute Bose gas with hard-sphere interactions. The dotted line is the corresponding isotherm for the free Bose gas at the same T.

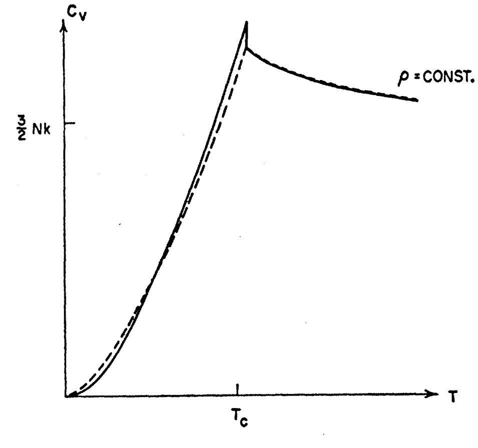

FIG. 3. Schematic C_v-T diagram for a dilute Bose gas with hard-sphere interactions. The dotted line is the corresponding curve for the free Bose gas at the same ρ.

In the treatment of the binary collision method it is pointed out that if we write the virial type expansion in the form

$$\lambda^3 p/\kappa T=\sum_{l=0}^{\infty}(a/\lambda)^l f_l(z), \tag{79}$$

then as $z\rightarrow 1_-$ the function $f_l(z)$ becomes singular for all values of $l\geqq 2$. Furthermore, it is proved that if we set

$$z=e^{-\epsilon},$$

then as $\epsilon\rightarrow 0_+$, f_l can be expanded as a series. For $l\geqq 2$, we have

$$f_l(z)=\epsilon^{-l}[A_l\epsilon^{\frac{3}{2}}+B_l\epsilon^2+C_l\epsilon^{\frac{5}{2}}+\cdots], \tag{80}$$

where A_l, B_l, etc., are independent of ϵ. Thus we may regroup the series in (79) and write

$$\lambda^3 p/\kappa T=1.342-(2.612)\epsilon-2(2.612)^2(a/\lambda) +\epsilon^{\frac{3}{2}}\mathbf{F}_{\frac{3}{2}}(a/\epsilon\lambda)+\epsilon^2\mathbf{F}_2(a/\epsilon\lambda)+\cdots, \tag{81}$$

where

$$\mathbf{F}_{\frac{3}{2}}(x)=\sum_{l=0}^{\infty}A_l x^l,$$
$$\mathbf{F}_2(x)=\sum_{l=0}^{\infty}B_l x^l,\ \text{etc.} \tag{82}$$

In (82), A_0 and B_0 are coefficients of $\epsilon^{\frac{3}{2}}$ and ϵ^2 in the series expansion for f_0 for small ϵ; A_1 and B_1 are the corresponding coefficients of $\epsilon^{\frac{1}{2}}$ and ϵ in the series expansion for f_1. The other A_l and B_l are defined by (80). These functions can be explicitly calculated by using the binary collision method. They are found to be

$$\mathbf{F}_{\frac{3}{2}}(a/\lambda\epsilon)=\tfrac{4}{3}\pi^{\frac{1}{2}}[1+4(2.612)a/\lambda\epsilon]^{\frac{3}{2}},$$

and (83)

$$\mathbf{F}_2(a/\lambda\epsilon)=B_0+B_1(a/\lambda\epsilon)+B_2(a/\lambda\epsilon)^2,$$

---

[8] Some results obtained with the binary collision method have been summarized in T. D. Lee and C. N. Yang, Phys. Rev. **105**, 1119 (1957). Notice that Eq. (5) of this reference was incorrect. It should read like Eqs. (70) and (71) of the present paper.

where

$$B_0=-0.730,$$
$$B_1=-2[4\pi+2(1.460)(2.612)],$$
$$B_2=-32\pi(2.612)-8(1.460)(2.612)^2+8F(z=1),$$
$$B_l=0,\quad \text{for}\quad l\geqq 3.$$

Thus, we find that $\lambda^3 p/\kappa T$ is *regular* at $\epsilon=0$ and that the singularity occurs at

$$\epsilon=-4(2.612)(a/\lambda)+O[(a/\lambda)^{\frac{3}{2}}], \tag{84}$$

which is identified as the transition point. The pressure and density at the transition point are given by (81):

$$\lambda^3(p_c/\kappa T)=1.342+2(2.612)^2(a/\lambda)+O[(a/\lambda)^{\frac{3}{2}}],$$

and

$$\lambda^3\rho_c=2.612+O(a/\lambda),$$

which are identical with those obtained in Sec. 7. We remark that it is indeed gratifying to find the results obtained in Sec. 7 not only agree with the virial-type expansion to order (a/λ) for all values of $z<1$, but also agree with the sum of the most singular part of $(a/\lambda)^l \times f_l(z)$ (including all values of l) as z is near 1.

9. DISCUSSIONS

We make a few remarks in this section about the present paper.

(i) The general line of reasoning described in Sec. 2 and developed in detail in the subsequent sections is also applicable to those states for which there is an incomplete but macroscopic occupation of a state of momentum $\mathbf{k}\neq 0$. Such states lead to superfluid flows and will be discussed in detail in a subsequent paper. For equilibrium thermodynamics, however, they are of no importance.

(ii) From the energy spectrum (18), we find the velocity of phonons of very long wavelength to be $(16\pi a\rho\xi)^{\frac{1}{2}}$. Thus, if the system is in thermodynamical equilibrium, the velocity of long-wavelength phonons has a statistical value $\bar{v}_{\text{phonon}}$, given by

$$\bar{v}_{\text{phonon}}=(16\pi a\rho\bar{\xi})^{\frac{1}{2}}, \tag{85}$$

which varies from $(16\pi a\rho)^{\frac{1}{2}}$ at $T=0$ to zero at the critical temperature. The interesting relationship between $\bar{v}_{\text{phonon}}$ and the macroscopic sound velocities will also be discussed in detail in the subsequent paper.

(iii) In Sec. 2, it was pointed out that for a dilute system of hard spheres one need only include those off-diagonal matrix elements of V for which two of the four occupation numbers $n_\alpha\ n_\beta\ n_\mu\ n_\nu$ are of the order of a finite fraction of N. The inclusion of the other off-diagonal matrix elements of V contribute to higher order corrections in energy. They also give rise to the scattering of the phonons and to the decay of a single phonon into two or three phonons of longer wavelengths. Let $\mathbf{k}$ be the momentum of the initial phonon and $\mathbf{k}_1$, $\mathbf{k}_2$ that of the final two. These momenta are related by

$$\mathbf{k}=\mathbf{k}_1+\mathbf{k}_2,$$

and (86)

$$k(k+16\pi a\xi\rho)^{\frac{1}{2}}=k_1(k_1^2+16\pi a\xi\rho)^{\frac{1}{2}}+k_2(k_2^2+16\pi a\xi\rho)^{\frac{1}{2}}.$$

Summing over all final states of $\mathbf{k}_1$, $\mathbf{k}_2$ we find the mean life τ of a phonon to be[9] (at $T\cong 0$)

$$\tau=(160\pi/3)\rho k^{-5}\quad\text{for}\quad k\ll(8\pi a\rho)^{\frac{1}{2}},$$

and (87)

$$\tau=(16\pi a^2\rho k)^{-1}\quad\text{for}\quad k\gg(8\pi a\rho)^{\frac{1}{2}}.$$

As is expected, the smaller the value of a the longer is the mean life.

The existence of these lifetimes throws new light on the nature of the "eigenstates" that were obtained in Sec. 3. Strictly speaking, these states are not eigenstates of the entire Hamiltonian. Transitions between them take place because of the decay, recombination and scattering of the phonons. The fact that one obtains states which are not eigenstates of the Hamiltonian is not really surprising. In fact, the exact eigenstates of the system are boundary-sensitive and are of no great physical interest. Furthermore, to the lowest order in a the approximate eigenstates give the equilibrium thermodynamical properties of the system. The situation is quite similar to a system of one hydrogen atom and the electromagnetic field: The excited states, $2s$, $2p$, etc., of an isolated hydrogen atom do not correspond to any real eigenstates of the system. However, if one neglects high-order terms in the fine structure constant, the eigenstate of the system becomes the product states of the free electromagnetic field and the isolated hydrogen atom. One can then compute the approximate thermodynamical behavior of the system using these metastable states.

(iv) We have seen that the presence of hard-sphere interactions for a dilute Bose gas gives rise to, on the one hand, phonon excitations which are superposable collective modes (i.e., that behave approximately as independent free modes), and also on the other hand, interactions between these modes which cause their scattering and their instability. It seems extremely plausible that the existence of certain superposable excitations that scatter and decay is a general characteristic of any nonlinear quantum mechanical system with a large number of degrees of freedom. In such a system, then, the problem of the interactions and the instability of the excitations and the problem of the very existence of these excitations must both go back to the nonlinearity of the original system, and cannot be separately understood.

ACKNOWLEDGMENT

The authors wish to thank the Brookhaven National Laboratory for the hospitality extended them during

---

[9] Details will be published in a subsequent communication.

their stay at Brookhaven in the Spring of 1958, when this paper was written.

APPENDIX

In this Appendix we shall study the behavior of a *model* whose energy spectrum is given *exactly* as

$$E=4\pi a\rho N[1+(1-\xi)^2]+\sum m_{\mathbf{k}}\omega_k, \tag{A1}$$

where

$$N^{-1}\sum_{\mathbf{k}\neq0} m_{\mathbf{k}}=(1-\xi)+O(N^{-1}),$$

and

$$\omega_k=k(k^2+16\pi a\xi\rho)^{\frac{1}{2}}.$$

To the first order in (a/λ) [for $\rho a^3\ll1$] the thermodynamical functions E, S, p, etc., of this system have been calculated in the text. These first-order results are the same as that of a dilute system of hard spheres obeying Bose statistics. To higher orders in (a/λ) the thermodynamical functions of a physical dilute system of hard spheres are not expected to be the same as that of this model. In fact, we shall show that if we take this model seriously and evaluate the partition function to higher orders in (a/λ) the resulting $p-V$ diagram exhibits unphysical behavior of the Van der Waals type. In particular, the results of the *partition function* of this model show that as one follows the isotherm from the gaseous phase to the liquid phase there is a sudden drop of pressure. This discontinuity of pressure occurs at a critical density

$$\rho_c=\lambda^{-3}(2.612)-(9.63)\lambda^{-3}(a/\lambda)+O[a^2/\lambda^5], \tag{A2}$$

with an amount

$$p_d-p_g=-(29.3)\kappa T\rho_c(a/\lambda)^2, \tag{A3}$$

where p_d and p_g are, respectively, the pressures in the degenerate phase and in the gaseous phase as the density approaches ρ_c.

On the other hand, one may use the *grand partititon function*, instead of the partition function, then the corresponding $p-V$ diagram would exhibit a flat portion. There will not be any discontinuity in pressure, but instead a discontinuity of density with the density ρ_α of the degenerate phase different from the gas density ρ_g. Both ρ_d and ρ_g differ from $\lambda^{-3}(2.612)$ by an amount $O(a/\lambda^4)$. This discontinuity of density occurs at a pressure

$$\lambda^3 p_c/\kappa T=1.342+(2.612)^2(2a/\lambda)+O[(a/\lambda)^2]. \tag{A4}$$

To prove (A2), (A3), and (A4), let us first consider the partition function. It is necessary to investigate in the (ξ,ζ) plane the detailed behavior of the curves $\xi=\xi(\rho,\zeta)$ [Eq. (27)] and to find the maximum value of $\Omega^{-1}\ln Q(\xi)$ along these curves for fixed values of ρ. The functional form of $\Omega^{-1}\ln Q(\xi)$ is given by Eq. (26). We notice that at $\xi=0$ and $\zeta<1$

$$\frac{\partial}{\partial\xi}[\Omega^{-1}\ln Q(\xi)]<0. \tag{A5}$$

Since ξ cannot be less than 0, the points with $\xi=0$ and $\zeta<1$ always correspond to local maxima of $\Omega^{-1}\ln Q(\xi)$. It is easy to show that for low density,

$$[\rho\lambda^3-(2.612)]<O(a/\lambda), \tag{A6}$$

these local maxima are also absolute maxima of $\Omega^{-1}\ln Q(\xi)$. The above condition [Eq. (A6)] is satisfied in the gaseous region. The most probable value of ξ in the gaseous region is, then,

$$\xi=0. \tag{A7}$$

However, as we increase density such that

$$[\rho\lambda^3-(2.612)]\sim O(a/\lambda), \tag{A8}$$

then these local maxima may not be the absolute maxima of $\Omega^{-1}\ln Q(\xi)$.

To investigate the detail change of ξ in the liquid phase near transition, it is necessary to calculate the integrals $\Omega^{-1}\ln Q(\xi)$ and $(1-\xi)\rho$ [Eqs. (26) and (27)] to very high orders in (a/λ). Let us write

$$\zeta=e^{-\epsilon}. \tag{A9}$$

It is convenient to define a parameter x,

$$x\equiv\epsilon/(2a\xi\rho\lambda^2). \tag{A10}$$

Equations (26) and (27) can then be written as

$$\begin{aligned}\Omega^{-1}\ln Q(\xi)=\lambda^{-3}g_{\frac{5}{2}}(\zeta)-4\pi a\rho^2\beta[1+(1-\xi)^2]+(1-\xi)\rho\epsilon\\ -2a\xi\rho\lambda^{-1}g_{\frac{3}{2}}(\zeta)+(2a\xi\rho)^{\frac{3}{2}}B(x)\\ +\tfrac{3}{2}(2a\xi\rho)^2\lambda[g_{\frac{1}{2}}(\zeta)-(\pi/\epsilon)^{\frac{1}{2}}]+O[(a\xi)^{\frac{5}{2}}],\end{aligned} \tag{A11}$$

and

$$\begin{aligned}(1-\xi)\rho=\lambda^{-3}g_{\frac{3}{2}}(\zeta)+\lambda^{-2}(2a\xi\rho)^{\frac{1}{2}}A(x)\\ -2a\xi\rho\lambda^{-1}[g_{\frac{1}{2}}(\zeta)-(\pi/\epsilon)^{\frac{1}{2}}]+O[(a\xi)^2],\end{aligned} \tag{A12}$$

where $A(x)$ and $B(x)$ are defined as

$$A(x)\equiv\frac{2}{\sqrt{\pi}}\int_0^\infty\frac{t}{x+t}\left\{\left[\frac{(t^2+1)^{\frac{1}{2}}-1}{t^2+1}\right]^{\frac{1}{2}}-t^{-\frac{1}{2}}\right\}dt. \tag{A13}$$

and

$$B(x)\equiv\frac{2}{\sqrt{\pi}}\int_0^\infty\frac{1}{x+t}\{\tfrac{2}{3}[(t^2+1)^{\frac{1}{2}}-1]^{\frac{3}{2}}-\tfrac{2}{3}t^{\frac{3}{2}}+t^{\frac{1}{2}}\}dt. \tag{A14}$$

The functions $A(x)$ and $B(x)$ satisfy the relation

$$dB/dx=-A(x)-(\pi/x)^{\frac{1}{2}}. \tag{A15}$$

The integral $A(x)$ can be evaluated explicitly. It is

$$\begin{aligned}A(x)=-4(2/\pi)^{\frac{1}{2}}+2(\pi x)^{\frac{1}{2}}-4x[\pi(x^2+1)]^{-\frac{1}{2}}\\ \times[1+(x^2+1)^{\frac{1}{2}}]^{\frac{1}{2}}\left\{\tan^{-1}\left(\frac{1-x+(x^2+1)^{\frac{1}{2}}}{\sqrt{2}[1+(x^2+1)^{\frac{1}{2}}]^{\frac{1}{2}}}\right)\right.\\ +\tan^{-1}\left(\frac{x}{\sqrt{2}[1+(x^2+1)^{\frac{1}{2}}]^{\frac{1}{2}}}\right)\\ -\tfrac{1}{2}x[1+(x^2+1)^{\frac{1}{2}}]^{-\frac{1}{2}}\ln(x^{-1}[1+(x^2+1)^{\frac{1}{2}}]\\ \left.+\sqrt{2}x^{-1}[1+(x^2+1)^{\frac{1}{2}}]^{\frac{1}{2}})\right\}.\end{aligned} \tag{A16}$$

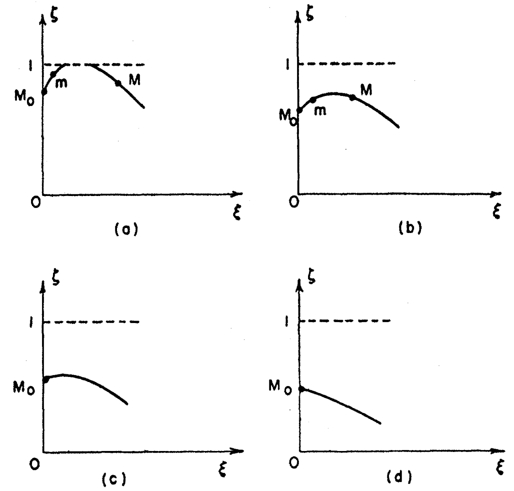

FIG. 4. Schematic plots of $\xi=\xi(\zeta,\rho)$ [Eq. (A19)] for the model (discussed in the Appendix). Figures 4(a), 4(b), 4(c), 4(d), are for the density ranges (a) $0<-\delta\rho<(16/\pi)(a/\lambda^4)$, (b) $(16/\pi)\times(a/\lambda^4)<-\delta\rho<(10.4)(a/\lambda^4)$, (c) $(10.4)(a/\lambda^4)<-\delta\rho<4\pi(a/\lambda^4)$, and (d) $-\delta\rho>4\pi(a/\lambda^4)$, respectively. The points m and M denote the minimum and maximum of $\Omega^{-1}\ln Q(\xi)$ along these curves.

Let us define

$$\delta\rho=\rho-\lambda^{-3}(2.612). \tag{A17}$$

In the following we shall consider only the region near the transition point, i.e.,

$$\lambda^3\delta\rho\sim O(a/\lambda),$$

and

$$\xi\sim O(a/\lambda). \tag{A18}$$

For these ranges it is easy to see that Eq. (A12) becomes

$$-\xi\rho+\delta\rho=-\lambda^{-3}2(\pi\epsilon)^{\frac{1}{2}} +\lambda^{-2}(2a\xi\rho)^{\frac{1}{2}}A(x)+O(a^2/\lambda^5). \tag{A19}$$

In Fig. 4 we plot the curves $\xi=\xi(\rho,\zeta)$ in the (ξ,ζ) plane for the various values of $\delta\rho$. In the following we discuss the different physical conditions for these four figures: 4(a), 4(b), 4(c), and 4(d).

1. In Fig. 4(a), we plot schematically a typical curve $\xi=\xi(\zeta,\rho)$ [Eq. (A19)] for a ρ value which satisfies

$$0<-\delta\rho<16\pi^{-1}(a/\lambda^4). \tag{A20}$$

We see that since

$$\zeta\leqq 1,$$

this curve is broken into two pieces. The maximum value of $\Omega^{-1}\ln Q(\xi)$ along this curve can be found by setting the derivative of $\Omega^{-1}\ln Q(\xi)$ with respect to ξ equal to zero,

$$\frac{\partial}{\partial\xi}[\Omega^{-1}\ln Q(\xi)]=0. \tag{A21}$$

Upon using Eq. (A11), (A21) becomes

$$\epsilon=(2a)^{\frac{3}{2}}(\xi\rho)^{\frac{1}{2}}[\tfrac{3}{2}B+(1+x)A+(\pi x)^{\frac{1}{2}}]. \tag{A22}$$

Combining with (A19), (A22) yields two roots ξ_m and ξ_M corresponding to a minimum and a maximum of $\Omega^{-1}\ln Q(\xi)$, respectively. In Fig. 4(a) we denote these two points as m and M. As explained before, the point M_0 which denotes $\xi=0$ corresponds to a local maximum. However, by using the above expressions, it can be proved that

$$\Omega^{-1}\ln Q(\xi_M)>\Omega^{-1}\ln Q(\xi=0). \tag{A23}$$

Thus the most probable value is

$$\bar{\xi}=\xi_M.$$

Figure 4(a), then, corresponds to the degenerate phase.

2. In Figs. 4(c) and 4(d) we plot the curves $\xi=\xi(\rho,\zeta)$ for

$$10.4(a/\lambda^4)<-\delta\rho<4\pi(a/\lambda^4), \tag{A24}$$

and

$$-\delta\rho>4\pi(a/\lambda^4), \tag{A25}$$

respectively. In both cases, (A21) and (A19) yield only complex solutions for ξ. Consequently, along these curves

$$\frac{\partial}{\partial\xi}[\Omega^{-1}\ln Q(\xi)]<0. \tag{A26}$$

Thus we have

$$\bar{\xi}=0, \tag{A27}$$

provided

$$-\delta\rho>(10.4)(a/\lambda^4).$$

Figures 4(c) and 4(d), then, correspond to the gas phase.

3. In Fig. 4(b) we plot the curve $\xi=\xi(\zeta,\rho)$ for a density

$$16\pi^{-1}(a/\lambda^4)<-\delta\rho<10.4(a/\lambda^4). \tag{A28}$$

In this case (A21) and (A19) still determine two real roots ξ_m and ξ_M correspond to a minimum value and a maximum value of $\Omega^{-1}\ln Q(\xi)$. However, if

$$-\delta\rho<9.63(a/\lambda^4),$$

then we have

$$\Omega^{-1}\ln Q(\xi_M)>\Omega^{-1}\ln Q(\xi=0).$$

For densities with

$$-\delta\rho>9.63(a/\lambda^4),$$

we have

$$\Omega^{-1}\ln Q(\xi_M)<\Omega^{-1}\ln Q(\xi=0).$$

Consequently, we have for the most probable value of ξ,

$$\bar{\xi}=\xi_M \quad \text{for} \quad -\lambda^3\delta\rho<(9.63)(a/\lambda),$$

and

$$\bar{\xi}=0 \quad \text{for} \quad -\lambda^3\delta\rho>(9.63)(a/\lambda).$$

Thus at the critical density value,

$$\rho_c=\lambda^{-3}(2.612)-9.63(a/\lambda^4)+O(a^2/\lambda^5),$$

there is a discontinuity of $\bar{\xi}$ and a discontinuity of pressure.

(i) On the degenerate side, as the density $\rho\rightarrow\rho_c+$, the parameters ξ and x approach

$$\xi \rightarrow 4.23(a/\lambda), \tag{A29}$$

and

$$x \rightarrow 0.66. \tag{A30}$$

Correspondingly, $\Omega^{-1}\ln Q$ and the pressure p_d approach

$$\Omega^{-1}\ln Q \rightarrow [\lambda^{-3}(1.342) - 8\pi a\rho_c^2\beta - 23.6\lambda^{-3}(a/\lambda)^3], \tag{A31}$$

$$p_d \rightarrow (p_d)_c = \lambda^{-3}\kappa T(1.342) + 8\pi a\rho_c^2 - (36.7)(a/\lambda)^2\rho_c\kappa T. \tag{A32}$$

(ii) On the gaseous side, the parameter ξ is always given by

$$\xi = 0. \tag{A33}$$

As the density ρ approaches the critical value ρ_c, the pressure p_g and $\Omega^{-1}\ln Q$ approach

$$\Omega^{-1}\ln Q \rightarrow [\lambda^{-3}(1.342) - 8\pi a\rho_c^2\beta - (23.6)\lambda^{-3}(a/\lambda)^3], \tag{A34}$$

and

$$p_g \rightarrow (p_g)_c = \lambda^{-3}\kappa T(1.342) + 8\pi a\rho_c^2 - (7.4)(a/\lambda)^2\rho_c\kappa T.$$

Thus we find that as we change from the gas phase to the degenerate phase there is a sudden unphysical drop of the pressure of the order of $(a/\lambda)^2$,

$$(\rho_d)_c - (\rho_g)_c = -29.3(a/\lambda)^2\rho_c\kappa T. \tag{A35}$$

This shows that although to first order of (a/λ) the thermodynamical functions are correctly evaluated by using the energy spectrum [Eq. (A1)], the higher order terms of this model do not correspond to any real physical system.

On the other hand, one may use the grand partition function instead of the partition function, to calculate the thermodynamical functions for this model. It is easy to show that the use of the grand partition function leads to the well-known application of Maxwell's rule of equal area on the Van der Waals type isotherm obtained from the partition function. From the previous results for the partition function one finds that the resulting isotherm by using the grand partition function has no discontinuity in pressure, but, instead, a discontinuity of density

$$(\rho_d - \rho_g) \sim O(a/\lambda^4),$$

which occurs at a pressure p_c given by Eq. (A4).

PHYSICAL REVIEW VOLUME 112, NUMBER 5 DECEMBER 1, 1958

Suprathermal Particles. III. Electrons*

E. N. Parker

Enrico Fermi Institute for Nuclear Studies and the Department of Physics, University of Chicago, Chicago, Illinois

(Received July 25, 1958)

Certain phenomena in nature, such as the 50- to 100-kev electrons of the aurora, suggest that there are plasma-dynamical processes which can quickly transfer the translational energy of the ions in a plasma stream to the electrons (some 20 kev/ion for a 2000-km/sec solar wind). It is shown that two interpenetrating streams of noncolliding and initially neutral plasma can achieve this energy transfer with a characteristic time comparable to $(M/m)^{\frac{1}{2}}$ times the plasma period. The process is closely analogous to the excitation of plasma oscillations by two interpenetrating electron streams, but of course proceeds to much greater electron energies because the ion components of the streams carry so much more kinetic energy than do the electron components. Hence, besides the auroral electrons, it is probably responsible for solar radio emission, rather than the electron streams implied in current theories.

Further, the process is probably the dominant interaction in shock fronts, particularly in astrophysical cases where neither direct collisions nor the existing weak magnetic fields can give sharp fronts. The characteristic thickness of a shock front in the solar wind is of the order of 10^4 cm due to the above plasma excitation whereas the Larmor radius of the ions, which would otherwise determine the shock thickness in the absence of collisions, is 100 km or more.

I. INTRODUCTION

We have previously noted the common appearance in nature of charged particles with energies very much in excess of the general thermal background.[1] Cosmic rays from interstellar space and from solar flares[2] represent the most extreme case of high ion energies. More moderate examples are the primary auroral protons[3] (with energies up to a few hundred kev) and the deuterons responsible for the neutron production observed in laboratory electrical discharges.[4,5] The soft x-rays observed by van Allen[6]

---

* Assisted in part by the Office of Scientific Research and the Geophysics Research Directorate, Air Force Cambridge Research Center, Air Research and Development Command, U. S. Air Force.

[1] E. N. Parker, Phys. Fluids 1, 171 (1958).

[2] Meyer, Parker, and Simpson, Phys. Rev. 104, 768 (1956).

[3] J. W. Chamberlain, Astrophys. J. 126, 245 (1957).

[4] Thonemann, Butt, Carruthers, Dellis, Fry, Gibson, Harding, Lees, McWhirter, Pease, Ramsden, and Ward, Nature 181, 217 (1958).

[5] S. Colgate, *Lockheed Symposium on Magnetohydrodynamics, Palo Alto, California, December 16, 1957* (to be published).

[6] Meredith, Gottlieb, and Van Allen, Phys. Rev. 97, 201 (1955).